J|A|C|S
ARTICLES
Published on Web 09/02/2006

π-Complex Structure of Gaseous Benzene−NO Cations Assayed by IR Multiple Photon Dissociation Spectroscopy

Barbara Chiavarino,[†] Maria Elisa Crestoni,[†] Simonetta Fornarini,*[,†] Joel Lemaire,[‡] Philippe Maître,*[,‡] and Luke MacAleese[‡]

Contribution from the Dipartimento di Studi di Chimica e Tecnologia delle Sostanze Biologicamente Attive, Università di Roma "La Sapienza", P.le A. Moro 5, I-00185 Roma, Italy, and Laboratoire de Chimie Physique, UMR8000 Université Paris-Sud 11, Faculté des Sciences d' Orsay, Bâtiment 350, 91405 Orsay Cedex, France

Received May 29, 2006; E-mail: simonetta.fornarini@uniroma1.it

Abstract: $[C_6H_6NO]^+$ ions, in two isomeric forms involved as key intermediates in the aromatic nitrosation reaction, have been produced in the gas phase and analyzed by IR multiple photon dissociation (IRMPD) spectroscopy in the 800−2200 cm^{-1} fingerprint wavenumber range, exploiting the high fluence and wide tunability of a free electron laser (FEL) source. The IRMPD spectra were compared with the IR absorption spectra calculated for the optimized structures of potential isomers, thus allowing structural information on the absorbing species. $[C_6H_6NO]^+$ ions were obtained by two routes, taking advantage of the FEL coupling to two different ion traps. In the first one, an FT-ICR mass spectrometer, a sequence of ion−molecule reactions was allowed to occur, ultimately leading to an NO^+ transfer process to benzene. The so-formed ions displayed IRMPD features characteristic of a [benzene,NO]$^+$ π-complex structure, including a prominent band at 1963 cm^{-1}, within the range for the N−O bond stretching vibration of NO (1876 cm^{-1}) and NO^+ (2344 cm^{-1}). A quite distinct species is formed by electrospray ionization (ESI) of a methanol solution of nitrosobenzene. The ions transferred and stored in a Paul ion trap showed the IRMPD features of substituent protonated nitrosobenzene, the most stable among conceivable $[C_6H_6NO]^+$ isomers according to computations. It is noteworthy that IRMPD is successful in allowing a discrimination between isomeric $[C_6H_6NO]^+$ species, whereas high-energy collision-induced dissociation fails in this task. The [benzene,NO]$^+$ π-complex is characterized by IRMPD spectroscopy as an exemplary noncovalent ionic adduct between two important biomolecular moieties.

Introduction

Cationic benzene−NO complexes are important species for various reasons. They are recognized as intermediates in the mechanism of aromatic nitrosation. Though belonging to the vast family of electrophilic aromatic substitution (EAS) reactions, probably the most studied processes in organic chemistry,[1] the mechanistic details of aromatic nitrosation have been elucidated only recently.[2] Within the framework of the general reaction pathway for EAS reactions, a key role in aromatic nitrosation is assigned to a π-complex ($E^+ = NO^+$ in eq 1).

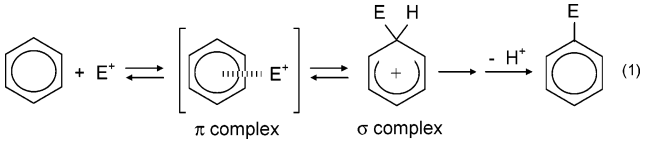

(1)

Indeed nitrosated π-complexes are considered to be the intermediates affording both substitution products as well as one-electron oxidation products, namely, the aromatic radical cation.[2a] These π-complexes were isolated in condensed phases and characterized by both X-ray crystallography and IR spectroscopic analysis of the NO stretching frequency.[2a] The IR spectroscopic features were indicative of a degree of charge transfer imparting them the character of electron donor−acceptor complexes. In particular, the N−O stretching vibration of [benzene,NO]$^+$ (ν_{NO} = 2075 cm^{-1} in nitromethane solution) suggested a degree of charge transfer of 0.52,[2a] implying that the aromatic moiety takes on a substantial amount of positive charge. This result is a consequence of the close values of the ionization energies of benzene and NO, IE = 9.24 and 9.26 eV,[3] respectively. The computed potential energy diagram for the electrophilic aromatic nitrosation of benzene by NO^+ has displayed similar features from comparative approaches.[2f] The

[†] Università di Roma "La Sapienza".
[‡] Université Paris-Sud 11.

(1) (a) Smith, M. B.; March, J. *March's Advanced Organic Chemistry: Reactions, Mechanisms, and Structure*; Wiley: New York, 2000. (b) Taylor, R. *Electrophilic Aromatic Substitution*; Wiley: New York, 1990. (c) Olah, G. A.; Malhotra, R.; Narang, S. C. *Nitration: Methods and Mechanisms*; VCH: New York, 1989.
(2) (a) Kim, E. K.; Kochi, J. K. *J. Am. Chem. Soc.* **1991**, *113*, 4962−4974. (b) Bockman, T. M.; Karpinski, Z. J.; Sankararaman, S.; Kochi, J. K. *J. Am. Chem. Soc.* **1992**, *114*, 1970−1985. (c) Bosch, E.; Kochi, J. K. *J. Org. Chem.* **1994**, *59*, 5573−5586. (d) Hubig, S. M.; Kochi, J. K. *J. Am. Chem. Soc.* **2000**, *122*, 8279−8288. (e) Rosokha, S. V.; Kochi, J. K. *J. Am. Chem. Soc.* **2001**, *123*, 8985−8999. (f) Gwaltney, S. R.; Rosokha, S. V.; Head-Gordon, M.; Kochi, J. K. *J. Am. Chem. Soc.* **2003**, *125*, 3273−3283.
(3) Lias, S. G. Ionization Energy Evaluation. In *NIST Chemistry WebBook*, NIST Standard Reference Database Number 69; Linstrom, P. J., Mallard, W. G., Eds.; National Institute of Standards and Technology: Gaithersburg, MD, 2005 (http://webbook.nist.gov).

key intermediate was found to lie in a broad single minimum corresponding to the [benzene,NO]$^+$ π-complex, formed from the free reactants in a barrierless association process. This intermediate may evolve to the nitrosated product via a rate-limiting transition state which resembles a σ-complex intermediate. The process may be viewed as a migratory insertion of nitrogen into the C−H bond, as depicted by density functional B3LYP calculations.[4] Skokov and Wheeler also found that the progress of hydrogen migration involved in this transition state accounts for a calculated kinetic isotope effect of $k_H/k_D = 11.5$ for benzene,[4] in close agreement with experiment. The low rates of aromatic nitrosation are thus assigned to the significant barrier accompanying the conversion of the π-complex to the N-protonated nitrosoderivative.[2f,4] The formation of N-protonated nitrosobenzene as the end ionic product of the nitrosation reaction is in accordance with the site-specific proton affinities of nitrosobenzene.[5] Protonation of the nitrogen atom is preferred over oxygen protonation, and ring protonation is still less favorable, yielding lower proton affinities than in parent benzene. The *ipso*-protonated isomer is likely not a minimum on the potential energy surface.[2f,6] Attempts to localize this stationary point led to the π-complex with a stretching of the C−N bond and a displacement of NO toward the π-position, according to B3LYP/6-31+G** calculations.[6]

Seminal studies on the nitrosation reaction in the gas phase are due to Reents and Freiser, who compared the reactivity properties of the cationic species formed by nitrosation of benzene and protonation of nitrosobenzene using ICR mass spectrometry.[7] The photodissociation spectrum of gaseous [benzene,NO]$^+$ ions and their NO$^+$ donor activity toward pyridine supported a π-complex structure, whereas protonated nitrosobenzene behaved as a substituent protonated species able to protonate pyridine. The reactivity probe with pyridine was also used to assign a π-complex structure to [benzene,NO]$^+$ ions obtained by alternative routes, such as the reaction of protonated benzene with neutral alkyl nitrites and nitrous acid.[6,8] Ions formally corresponding to [benzene,NO]$^+$ have been obtained also by NO chemical ionization (CI)[9] and in a selected ion flow tube apparatus,[10] though their structure has not been further inquired. In a recent study by Grabowy and Mayer, NO chemical ionization has been recognized as a possible source of excited electronic states for the ionic complexes with aromatic compounds arising from the reaction of triplet NO$^+$,[11] co-produced in the ion source with ground state singlet NO$^+$.[9b] Regarding the structural characterization of [benzene,NO]$^+$ ions, collision-induced dissociation (CID) mass spectrometry did not prove to be diagnostic in distinguishing between nitrosated benzene and protonated nitrosobenzene. However, the mass spectrum of metastable [benzene,NO]$^+$ cluster ions showed signals at *m*/*z* 78 and 30 corresponding to ionized benzene and NO$^+$, respectively, consistent with a π-complex between NO$^+$ and benzene.[11] A similar conclusion was reached by neutralization−reionization (NR) mass spectrometry of [benzene,NO]$^+$ ions, showing no recovery signal corresponding to survivor ions, in contrast with an intense recovery signal observed in the NR spectrum of protonated nitrosobenzene.[6] However, purely mass spectrometric approaches to structural elucidation of a selected ionic species, such as CID, metastable ion analysis, NR mass spectrometry, and ion−molecule reactions, are based on unimolecular or bimolecular reactivity behavior, namely, on processes involving significant perturbation of the species being assayed.

A spectroscopic technique would circumvent this problem to a large extent. In this paper, a recent approach for the IR spectroscopic characterization of ions is exploited to probe the structure and bonding features of the gaseous species of interest. IR spectroscopy of mass selected ions of increasing molecular size has made continuous and significant progress in recent years, though facing inherent problems due to the typically low number density and to their specific formation pathway.[12] The absorption of IR photons can be probed by the dissociation process that may follow if the energy gained raises the internal energy of the ion up to a dissociation threshold. In the highly diagnostic so-called fingerprint region of the IR spectrum, this limit may require the absorption of several photons as ensured by powerful radiation sources. Tunability is a second requisite that is called for the investigation of an informative portion of the IR spectrum. Both conditions, high peak power and tunability, are fulfilled by the radiation provided by a free electron laser (FEL), and a wealth of valuable information on the IR spectroscopic features of gaseous ions is emerging from combined approaches based on mass spectrometric techniques for ion formation, trapping, and detection coupled with admittance of the FEL IR radiation and ensuing multiple photon absorption process by the selected ions. In this way, it became possible to uncover molecular properties of important ionic species, such as alkali metal tagged amino acids and peptides,[13] the protonated water dimer,[14] the radical cations of polycyclic aromatic hydrocarbons,[15] transition metal ion complexes,[16] and naked carbocations[17] addressing issues such as structure, bonding features, electronic state of a ligated metal ion, to name only a few.

The mechanism of resonant IR excitation of gaseous species by multiple photon absorption has been described[18] and theoretically investigated using numerical simulations.[15] The production of photofragments and their relative abundance with respect to intact parent ions is recorded as a function of the radiation

(4) Skokov, S.; Wheeler, R. A. *J. Phys. Chem. A* **1999**, *103*, 4261−4269.
(5) Eckert-Maksić, M.; Hodošček, M.; Kovacek, D.; Maksić, Z. B.; Primorac, M. *J. Mol. Struct. (THEOCHEM)* **1997**, *417*, 131−143.
(6) Dechamps, N.; Gerbaux, P.; Flammang, R.; Bouchoux, G.; Nam, P.-C.; Nguyen, M.-T. *Int. J. Mass Spectrom.* **2004**, *232*, 31−40.
(7) (a) Reents, W. D., Jr.; Freiser, B. S. *J. Am. Chem. Soc.* **1980**, *102*, 271−276. (b) Reents, W. D., Jr.; Freiser, B. S. *J. Am. Chem. Soc.* **1981**, *103*, 2791−2797.
(8) Cacace, F.; Ricci, A. *Chem. Phys. Lett.* **1996**, *253*, 184−188.
(9) (a) Daishima, S.; Iida, Y.; Kanda, F. *Org. Mass Spectrom.* **1991**, *26*, 486−492. (b) Williamson, A. D.; Beauchamp, J. L. *J. Am. Chem. Soc.* **1975**, *97*, 5714−5718.
(10) (a) Španěl, P.; Smith, D. *Int. J. Mass Spectrom.* **1998**, *181*, 1−10. (b) Smith, D.; Wang, T.; Španěl, P. *Int. J. Mass Spectrom.* **2003**, *230*, 1−9.
(11) Grabowy, J. A. D.; Mayer, P. M. *Eur. J. Mass Spectrom.* **2004**, *10*, 899−907.
(12) (a) Dunbar, R. C. *Int. J. Mass Spectrom.* **2000**, *200*, 571−589. (b) Duncan, M. A. *Int. J. Mass Spectrom.* **2000**, *200*, 545−569. (c) Bieske, E. J.; Dopfer, O. *Chem. Rev.* **2000**, *100*, 3963−3998. (d) White, E. T.; Tang, J.; Oka, T. *Science* **1999**, *284*, 135−137. (e) Hirota, E. *Chem. Rev.* **1992**, *92*, 141−173. (f) Stephenson, S. K.; Saykally, R. J. *Chem. Rev.* **2005**, *105*, 3220−3234. (g) Maier, J. P., Ed. *Ion and Cluster Ion Spectroscopy and Structure*; Elsevier: Amsterdam, 1989.
(13) (a) Kapota, C.; Lemaire, J.; Maître, P.; Ohanessian, G. *J. Am. Chem. Soc.* **2004**, *126*, 1836−1842. (b) Polfer, N. C.; Paizs, B.; Snoek, L. C.; Compagnon, I.; Suhai, S.; Meijer, G.; Von Helden, G.; Oomens, J. *J. Am. Chem. Soc.* **2005**, *127*, 8571−8579. (c) Oomens, J.; Polfer, N.; Moore, D. T.; van der Meer, L.; Marshall, A. G.; Eyler, J. R.; Meijer, G.; von Helden, G. *Phys. Chem. Chem. Phys.* **2005**, *7*, 1345−1348.
(14) (a) Asmis, K. R.; Pivonka, N. L.; Santambrogio, G.; Brümmer, M.; Kaposta, C.; Neumark, D. M.; Wöste, L. *Science* **2003**, *299*, 1375−1377. (b) Fridgen, T. D.; McMahon, T. B.; MacAleese, L.; Lemaire, J.; Maître, P. *J. Phys. Chem. A* **2004**, *108*, 9008−9010.

wavelength yielding an IR multiple photon dissociation (IRMPD) spectrum, reflecting the resonance-enhanced multiple photon absorption in correspondence with the active IR modes of the sampled species. In view of the complexity of the process, not yet understood in every detail, which comprises multiple photon absorption and intramolecular vibrational relaxation followed by a dissociation process, it is remarkable that according to growing evidence IRMPD spectra may display close analogy with the linear IR spectra reflecting the absorption of a single photon.[13−17] Typically, the unknown structure of a mass selected ion may thus be elucidated by comparing the experimental IRMPD spectrum with the IR spectra calculated for potential candidates.

Two ion traps coupled to the IR beam line of the FEL at the Centre Laser Infrarouge d'Orsay (CLIO, a European facility)[19] have been used in this work. The first one has been previously described in detail and is based on a movable FT-ICR mass spectrometer,[16f,20] The second ion trap is a commercial Paul-type ion trap instrument (Bruker Esquire) equipped with an electrospray ionization (ESI) ion source. A ZnSe optical window allows the radiation to enter the cell, where ions may be selected by ion ejection techniques, and submitted to multiple photon absorption. The relative performances of these experimental setups have been discussed recently.[21] The mass spectrum recorded at the end of the sequence reveals any photofragment ions possibly formed from the selected parent ion, the cell of the mass spectrometer acting as reaction vessel, ion trap, sampling, and detection area of the ion of interest.

In our view, $[benzene,NO]^+$ complexes deserve additional interest because they contain two important fragments performing fundamental functions in biochemistry. Benzene is the prototypical aromatic molecule partaking in cation−π interactions that concur in determining the structures of biomolecules.[22] Cation−π interactions are important forces in molecular recognition, and molecular systems have been designed with proper arrangement of benzene units that may act as ionophores and provide models for biological receptors.[23] NO is a key mediator in a great number of physiological processes as diverse as blood pressure regulation, platelet aggregation, immune defense, and neurotransmission.[24] The important role of NO and biochemical nitrosation reactions has prompted the development of extensive scales of intrinsic NO^+ affinities to series of model compounds in the gas phase.[7b,25] The present work is focused on the exemplary cationic complex between benzene and NO, aiming to provide unequivocal proof of the π-complex structure. To this end, the comparative examination of alternative structures that may result from the protonation of nitrosobenzene was undertaken and is also reported.

Experimental and Computational Section

1. IR FEL and MS Parameters. The details of the experimental apparatus are largely described, and only few major features are summarized.[16f,20b] The CLIO FEL is based on a 10−50 MeV electron linear accelerator in series with an undulator placed in an optical cavity.[19] The output allows continuous tunability in the $\Delta\lambda/\lambda = 2.5$ range for each electron energy and is delivered in trains of 8 μs long macropulses at a repetition rate of 25 Hz. Each macropulse contains 500 micropulses, the latter are only a few picoseconds long. A mean radiation power of 1 W corresponds to macropulse and micropulse energies of 40 mJ and 80 μJ, respectively. The IR radiation from the FEL operated at 42, 45, or 48 MeV was monitored for wavelength reading at each scan using a monochromator associated with a spiricon. In the first configuration adopted, the FEL laser light is directed into the cell of a movable FT-ICR mass spectrometer (MICRA)[20a] by a spherical mirror of 1 m focal length. The MICRA spectrometer is based on a 2 cm cubic cell placed within a compact 1.25 T magnet, where neutrals can be pulsed in and ionized. The temporal sequence of each experiment comprised the admission of methane (at 7.9×10^{-7} mbar), which was ionized and allowed to undergo ion−molecule reactions forming protonating ions. Delay times were allowed following the admission of isoamylnitrite (at 5.0×10^{-7} mbar) and then of benzene (at 5.0×10^{-7} mbar). The so-formed $[C_6H_6NO]^+$ ions were mass selected using resonant frequency ejection techniques and exposed to the FEL light for 1 s, with the irradiation time controlled by a fast electromechanical shutter. Excitation, detection, and quench of the ions in the cell completed the sequence, resulting in a mass spectrum from an ion signal accumulated over 4 scans.

Alternatively, an instrumental setup has been used that was developed and made available recently,[21] based on a Bruker Esquire 3000 plus quadrupole Paul ion trap mass spectrometer. A 0.7 mm hole drilled in the ring electrode allows for the irradiation of the ions with the IR FEL laser beam, focused using a 25 cm focal lens. The ions were isolated in the ion trap and subjected to the IR beam for one macropulse. The IRMPD was recorded in the 800−1800 cm^{-1} wavenumber range with the IR FEL operating at 42 MeV. In this configuration, ions of the same elemental composition, $[C_6H_6NO]^+$, have been produced in the gas phase by an ESI source. Solutions ranging in nitrosobenzene concentration from 10 to 50 μM in methanol were directly infused by a syringe pump at a flow rate of 4 μL min^{-1}. Noteworthy, the addition

(15) (a) Oomens, J.; Tielens, A. G. G. M.; Sartakov, B. G.; von Helden, G.; Meijer, G. *Astrophys. J.* **2003**, *591*, 968−985. (b) Oomens, J.; Van Roij, A. J. A.; Meijer, G.; von Helden, G. *Astrophys. J.* **2000**, *542*, 404−410.

(16) (a) Oomens, J.; Moore, D. T.; von Helden, G.; Meijer, G.; Dunbar, R. C. *J. Am. Chem. Soc.* **2004**, *126*, 724−725. (b) Moore, D. T.; Oomens, J.; Eyler, J. R.; von Helden, G.; Meijer, G.; Dunbar, R. C. *J. Am. Chem. Soc.* **2005**, *127*, 7243−7254. (c) Van Heijnsbergen, D.; von Helden, G.; Meijer, G.; Maître, P.; Duncan, M. A. *J. Am. Chem. Soc.* **2002**, *124*, 1562−1563. (d) Jaeger, T. D.; Van Heijnsbergen, D.; Klippenstein, S. J.; von Helden, G.; Meijer, G.; Duncan, M. A. *J. Am. Chem. Soc.* **2004**, *126*, 10981−10991. (e) Simon, A.; Jones, W.; Ortega, J.-M.; Boissel, P.; Lemaire, J.; Maître, P. *J. Am. Chem. Soc.* **2004**, *126*, 11666−11674. (f) Lemaire, J.; Boissel, P.; Heninger, M.; Mauclaire, G.; Bellec, G.; Mestdagh, H.; Simon, A.; Le Caer, S.; Ortega, J. M.; Glotin, F.; Maître, P. *Phys. Rev. Lett.* **2002**, *89*, 273002−273004. (g) Moore, D. T.; Oomens, J.; Eyler, J. R.; Meijer, G.; von Helden, G.; Ridge, D. P. *J. Am. Chem. Soc.* **2004**, *126*, 14726−14727. (h) Reinhard, B. M.; Lagutschenkov, A.; Lemaire, J.; Maître, P.; Boissel, P.; Niedner-Schatteburg, G. *J. Phys. Chem. A* **2004**, *108*, 3350−3355. (i) Dunbar, R. C.; Moore, D. T.; Oomens, J. *J. Phys. Chem. A* **2006**, *110*, 8316−8326. (j) Polfer, N. C.; Oomens, J.; Moore, D. T.; von Helden, G.; Meijer, G.; Dunbar, R. C. *J. Am. Chem. Soc.* **2006**, *128*, 517−525.

(17) (a) Chiavarino, B.; Crestoni, M. E.; Fornarini, S.; Lemaire, J.; MacAleese, L.; Maître, P. *ChemPhysChem* **2004**, *5*, 1679−1685. (b) Polfer, N.; Sartakov, B. G.; Oomens, J. *Chem. Phys. Lett.* **2004**, *400*, 201−205.

(18) von Helden, G.; van Heijnsbergen, D.; Meijer, G. *J. Phys. Chem. A* **2003**, *107*, 1671−1688.

(19) (a) Prazeres, R.; Glotin, F.; Insa, C.; Jaroszynski, D. A.; Ortega, J.-M. *Eur. Phys. J. D* **1998**, *3*, 87−93. (b) Glotin, F.; Ortega, J. M.; Prazeres, R.; Rippon, C. *Nucl. Instrum. Methods B* **1998**, *144*, 8−17.

(20) (a) Mauclaire, G.; Lemaire, J.; Boissel, P.; Bellec, G.; Heninger, M. *Eur. J. Mass Spectrom.* **2004**, *10*, 155−162. (b) Maître, P.; Le Caër, S.; Simon, A.; Jones, W.; Lemaire, J.; Mestdagh, H.; Heninger, M.; Mauclaire, G.; Boissel, P.; Prazeres, R.; Glotin, F.; Ortega, J.-M. *Nucl. Instrum. Methods Phys. Res. A* **2003**, *507*, 541−546.

(21) MacAleese, L.; Simon, A.; McMahon, T. B.; Ortega, J.-M.; Scuderi, D.; Lemaire, J.; Maître, P. *Int. J. Mass Spectrom.* **2006**, *249*−*250*, 14−20.

(22) (a) Ma, J. C.; Dougherty, D. A. *Chem. Rev.* **1997**, *97*, 1303−1324. (b) Dougherty, D. A. *Science* **1996**, *271*, 1163−1168. (c) Ruan, C.; Rodgers, M. T. *J. Am. Chem. Soc.* **2004**, *126*, 14600−14610.

(23) (a) Koyanagi, G. K.; Bohme, D. K. *Int. J. Mass Spectrom.* **2003**, *227*, 563−575. (b) Choi, H. S.; Suh, S. B.; Cho, S. J.; Kim, K. S. *Proc. Natl. Acad. Sci. U.S.A.* **1998**, *95*, 12094−12099. (c) Gokel, J. W.; Barbour, L. J.; Ferdani, R.; Hu, J. *Acc. Chem. Res.* **2002**, *35*, 878−886.

(24) (a) Pfeiffer, S.; Mayer, B.; Hemmens, B. *Angew. Chem., Int. Ed.* **1999**, *38*, 1714−1731. (b) Ignarro, L. J. *Angew. Chem., Int. Ed.* **1999**, *38*, 1882−1892. (c) Furchgott, R. F. *Angew. Chem., Int. Ed.* **1999**, *38*, 1870−1880. (d) Murad, F. *Angew. Chem., Int. Ed.* **1999**, *38*, 1856−1868. (e) Gross, S. S. *Nature* **2001**, *409*, 577−578. (f) Lipton, S. A. *Nature* **2001**, *413*, 118−121.

(25) Cacace, F.; De Petris, G.; Pepi, F. *Proc. Natl. Acad. Sci. U.S.A.* **1997**, *94*, 3507−3512.

of acids, such as acetic acid, to the methanol solution aiming to improve the yield of protonated nitrosobenzene was found to have a detrimental effect, possibly due to substrate decomposition.

The IRMPD yield R is expressed as a function of the abundancies (I) of the parent and fragment ions as $R = -\ln\{I_{parent}/(I_{parent} + I_{fragment})\}$.

2. Computational Details. Molecular structures and relative energies for isomeric $[C_6H_6NO]^+$ species were calculated using hybrid density functional theory (B3LYP) and the 6-311+G** basis set using the Spartan '04 (revision 1.0.0; Wavefunction Inc.) software. Harmonic vibrational frequencies and IR absorption intensities obtained at the same level were used to interpret the IRMPD spectra. B3LYP calculations have already been reported for π-type complexes and N-protonated nitrosobenzene.[4,11] Furthermore, hybrid DFT methods, such as B3LYP, were found to perform well in describing IR absorption spectra in terms both of relative intensities and of absolute frequencies, provided that appropriate scaling factors are used.[26] Calculated IR frequencies are thus uniformly scaled by a factor of 0.98. However, in the present report, raw data are also given, as specifically stated wherever appropriate.

Results and Discussion

Formation of [Benzene,NO]$^+$ and Assay by IRMPD. [Benzene,NO]$^+$ ions are obtained by gas phase ion−molecule reactions in the FT-ICR cell, performing a NO^+ transfer process to neutral benzene. By this route, protonating ions formed by the chemical ionization of methane (CH_5^+ and $C_2H_5^+$) are allowed to react with isoamylnitrite ($(CH_3)_2CHCH_2CH_2ONO$). Protonated isoamylnitrite and its nitrosated fragment ions (RNO^+) may release NO^+ to benzene as depicted in eq 2, according to a known reaction pathway of protonated alkyl nitrites.[7a]

$$RNO^+ + C_6H_6 \rightarrow [\text{benzene,NO}]^+ + R \qquad (2)$$

A conceivable alternative route, the direct reaction of NO^+ with benzene, results in a charge exchange reaction under ICR conditions[7a,27] and was avoided also because of the possible contribution of excited electronic states of NO^+.[11] [Benzene,-NO]$^+$ ions isolated by conventional ion ejection techniques and submitted to irradiation by the FEL light are found to undergo a photodissociation process leading to $C_6H_6^{+\bullet}$ ions at m/z 78 (eq 3), to an extent depending on the IR radiation frequency.

$$[\text{benzene,NO}]^+ + n\text{h}\nu \rightarrow C_6H_6^{+\bullet} + NO^\bullet \qquad (3)$$

The photofragmentation yield R is plotted as a function of the wavenumber in Figure 1. The ensuing IRMPD spectrum shown in profile (a) spans the wavenumber range from 2200 to 1080 cm^{-1} and was recorded with a laser power varying from 0.74 to 1.14 W with the electron accelerator of the FEL operated at 48 MeV. The threshold energy for the dissociation process of eq 3 will depend on the specific features of the [benzene,-NO]$^+$ ions that are sampled. Experimental values for the NO^+ binding energy of benzene are somewhat scattered (131−194 kJ mol^{-1}).[7,25] Also, ab initio calculations yield a wide range of values, though the binding energy of a singlet [benzene,NO]$^+$ complex seems to converge to a value around 145 kJ mol^{-1} as the level of theory is improved.[11] Clearly, the dissociation

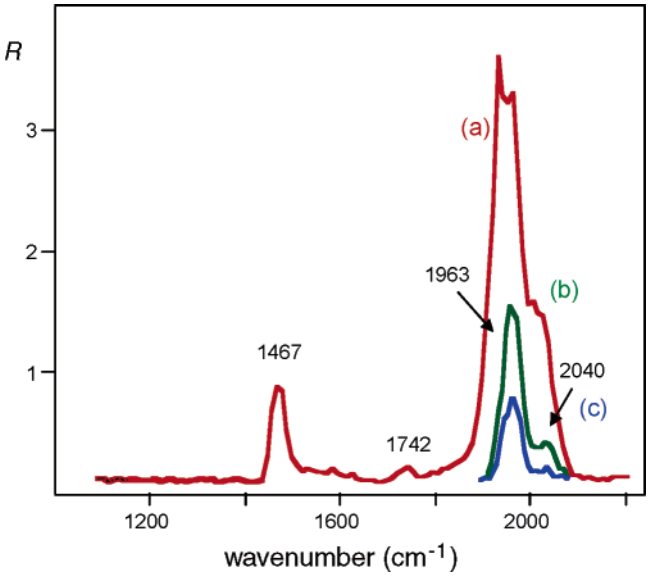

Figure 1. IRMPD spectrum of [benzene,NO]$^+$ ions obtained with full (a) and attenuated (b and c) laser power, as described in the text.

process would require activation by absorption of more than six photons at an exemplary photon wavenumber of 2000 cm^{-1}. Considering that the ionization energy of benzene is only 0.02 eV lower than that of NO$^\bullet$,[3] it is quite interesting that the only IRMPD photofragments are $C_6H_6^{+\bullet}$ ions and neutral NO$^\bullet$. The same fragment ion is by far the major product observed by UV photodissociation, collisionally induced dissociation, or metastable ion dissociation of [benzene,NO]$^+$ ions from various sources.[6,7a,11]

The IRMPD spectrum (profile (a)) shows two major features, a distinct band at 1467 cm^{-1} and a prominent absorption near 2000 cm^{-1}, the latter showing clear saturation behavior. Indeed, in correspondence with the pronounced maximum of this feature, the mass spectrum reveals that [benzene,NO]$^+$ ions are completely dissociated into $C_6H_6^{+\bullet}$ fragments. The IRMPD spectrum in the 2070−1915 cm^{-1} range has therefore been recorded with reduced laser power using attenuators. The IRMPD profiles (b) and (c) in Figure 1 were obtained at 150 and 50 mW, respectively. A maximum at 1963 cm^{-1} with a shoulder at 2040 cm^{-1} is now clearly discernible.

In order to extract structural information, the IRMPD spectrum of [benzene,NO]$^+$ ions can be compared with the calculated IR spectra of potential candidates. Vibrational spectra of crystalline complexes of the nitrosonium cation with arene donors have been studied, and the IR spectrum of a nitromethane solution containing both $NO^+PF_6^-$ and benzene was found to display a ν_{NO} stretching frequency at 2075 cm^{-1} ascribed to a [benzene,NO^+] electron donor−acceptor complex.[2a,e] However, a computational approach is adopted here in order to obtain a comprehensive set of IR spectra of plausible isomers against which the experimental IRMPD spectrum may be judged.

Calculated IR Spectra for $[C_6H_6NO]^+$ Isomers and Experimental IRMPD Spectrum of [Benzene,NO]$^+$. The optimized structures for isomers corresponding to the $[C_6H_6-NO]^+$ general formula have been obtained by B3LYP/6-311+G** calculations. Several of these structures have been described in previous reports.[2f,4−6,11] The data summarized in Table 1 present the relative energies of the various species, allowing a direct comparison, based on a common computational

(26) (a) Scott, A. P.; Radom, L. *J. Phys. Chem.* **1996**, *100*, 16502−16503. (b) Halls, M. D.; Velkovski, J.; Schlegel, H. B. *Theor. Chem. Acc.* **2001**, *105*, 413−421. (c) Sinha, P.; Boesch, S. E.; Gu, C.; Wheeler, R. A.; Wilson, A. K. *J. Phys. Chem. A* **2004**, *108*, 9213−9217.
(27) Lias, S. G.; Ausloos, P. *J. Am. Chem. Soc.* **1977**, *99*, 4831−4833.

Table 1. Relative Energies of $[C_6H_6NO]^+$ Isomers.

structure	E_{rel}[a]
$C_6H_6NO^+$ (**I**)	36.3
$C_6H_6NO^+$ (**II**)[b]	36.4
$C_6H_6NO^+$ (**III**)	56.8
o-NO−$C_6H_6^+$	139.3
m-NO−$C_6H_6^+$	139.3
p-NO−$C_6H_6^+$	141.6
$C_6H_5NOH^+$ (*cis*)	51.8
$C_6H_5NOH^+$ (*trans*)	8.5
$C_6H_5N(H)O^+$	0.0

[a] Relative energies in kJ mol^{-1} at 0 K. Calculations were performed at the B3LYP/6-311+G** level. ZPE corrections are included. [b] This species presents a pair of degenerate imaginary frequencies.

method. The first three entries pertain to π-complexes, the species that are recognized to form from several precursors both in the gas phase and in solution,[2,6−8,11] and the primary interest of the present study. The search for a [benzene,NO]$^+$ π-complex showed six equivalent geometries (**I** in Figure 2) with an almost unperturbed benzene ring coordinating the N-end of NO, in agreement with previous reports.[2f,4,6,11] The N−O bond is aligned on a plane containing two para C−H bonds and is slightly tilted (ca. 20°) with respect to the perpendicular axis crossing the center of the benzene ring. This distortion relieves the symmetrical geometry (**II** in Figure 2), a stationary point on the potential energy surface characterized by two degenerate imaginary frequencies. Structures **I** and **II** are quite close in energy due to the flatness of the potential energy surface. A parallel π-complex (**III** in Figure 2) is also found to lie in a local minimum. Once again, six equivalent geometries correspond to the N−O bond coplanar with a C−H bond, the N-end of NO pointing toward the carbon atom. It may be conceived that π-complex **III** should proceed by covalent ON−C bond formation toward a species resembling *ipso*-protonated nitrosobenzene. However, this hypothetical intermediate is not found to correspond to any stable species, rather evolving to π-complex **III** on geometry optimization. The reaction coordinate for aromatic nitrosation was suggested to proceed rather by NO insertion into a C−H bond, yielding N-protonated nitrosobenzene, though the process involves an energy barrier protruding above the energy level of the NO^+/benzene pair.[2f,4] N-Protonated nitrosobenzene, $C_6H_5N(H)O^+$, is the most stable species among the $[C_6H_6NO]^+$ isomers listed in Table 1, in agreement with the site-specific proton affinities obtained by the MP2(fc)/6-31G**//HF/6-31* + ZPE(HF/6-31G*) theoretical model.[5] As shown by the relative energies reported in Table 1, the carbon-protonated isomers are substantially less stable than $C_6H_5N(H)O^+$, whereas protonation at the oxygen atom of nitrosobenzene yields species (*cis*- or *trans*-$C_6H_5NOH^+$) endowed with comparable, though still lower, stability. The possible formation of any of these species under the current experimental conditions can be appropriately considered and eventually assessed by considering the computed IR spectra. To this end, Figure 3 displays the spectra of the [benzene,NO]$^+$ π-complexes **I** (a) and **III** (b), while Figure 4 includes the spectra of C-protonated isomers, namely, *o*-NO-$C_6H_6^+$ (c), *m*-NO-$C_6H_6^+$ (d), and *p*-NO-$C_6H_6^+$ (e), of the *cis* (f) and *trans* (g) isomers of $C_6H_5NOH^+$, and of $C_6H_5N(H)O^+$ (h) in the IR wavenumber range that was explored experimentally. In both Figures 3 and 4, the frequency values are corrected by the 0.98 scaling factor.

When the experimental IRMPD spectrum is examined against the computed IR spectra, it appears that the sampled $[C_6H_6NO]^+$ ion is best matched by the "perpendicular" π-complex **I** displaying a strongly active mode at 2075 cm^{-1} (N−O stretching) and a degenerate pair at 1471 cm^{-1} (in-plane carbon ring distortion). Whereas the latter mode nicely matches with the experimental IRMPD feature at 1467 cm^{-1}, the N−O stretching mode displays a large deviation with experiment, seemingly due to a failure of the scaling factor adopted. In order to gain an insight into the origin of this discrepancy, one may inspect the calculated IR spectrum and the experimental IRMPD features listed in Table 2, also reporting the raw frequency values, unaffected by any scaling. Table 2 also displays data pertaining to model molecules, allowing the experimental values of vibrational frequencies to be compared with the computed values at the same common level of theory. Thus, the in-plane carbon ring distortion vibrational modes (degenerate) reported at 1486 cm^{-1} for benzene in the gas phase[28] are found at 1511 cm^{-1} according to B3LYP/6-311+G** calculations. The ensuing factor of 0.983 (ratio exp/theory) is close to the one (0.977) relating the calculated IR frequency of 1501 cm^{-1} to the experimental IRMPD band of the sampled $[C_6H_6NO]^+$ ion at 1467 cm^{-1}, although a slight red shift in the experimental IRMPD frequencies with respect to the calculated absorption IR spectrum may be expected as an intrinsic consequence of the multiple photon process.[15] To find a model for the N−O bond stretching mode, one may refer to the experimental values reported for NO (1876 cm^{-1})[29] and for NO^+ (2344 cm^{-1}),[29,30] which are calculated at 1981 and 2490, respectively, at the B3LYP/6-311+G** level. The ensuing ratios of 0.947 and 0.941 are somewhat higher than the 0.927 factor that would bring the computed frequency of 2117 cm^{-1} for [benzene,NO]$^+$ to match with the IRMPD feature at 1963 cm^{-1} (see ratio exp/theory in Table 2). This result is not quite unexpected and is in line, for example, with the conclusion of Schlegel and co-workers, who showed that rather than scaling all the calculated vibrational frequencies using a uniform factor,[26b] a better agreement between experimental and calculated frequencies can be obtained using dual-scaling factors. In this way, one accounts for the fact that the high-energy stretching modes, typically above 1800 cm^{-1}, are more anharmonic and tend to lead to greater errors when treated by the harmonic approximation. In this regard, it is noteworthy that a scaling factor of ca. 0.94 should also be applied to the calculated (B3LYP/6-311G** level) N−O stretching frequencies of XNO compounds (X = H, F, Cl) in order to match the experimental frequencies.[31]

The agreement between computed IR spectra and experimental IRMPD spectra is also satisfactory when relative intensities are concerned. With the yield of the resonance-enhanced multiple photon dissociation process being the result of a complex sequence of events, it is remarkable that a general qualitative agreement is often found.[13−17] Also, the IRMPD yield should not be expected to display linear laser power dependence,

(28) Shimanouchi, T. Molecular Vibrational Frequencies. In *NIST Chemistry WebBook*, NIST Standard Reference Database Number 69; Linstrom, P. J., Mallard, W. G., Eds.; National Institute of Standards and Technology: Gaithersburg, MD, 2005 (http://webbook.nist.gov).
(29) Laane, J.; Ohlsen, J. R. *Prog. Inorg. Chem.* **1980**, *27*, 465−513.
(30) Ho, W. C.; Ozier, I.; Cramb, D. T.; Gerry, M. C. L. *J. Mol. Spectrosc.* **1991**, *149*, 559−561.
(31) *Computational Chemistry Comparison and Benchmark DataBase*, Release 12; National Institute of Standards and Technology: Gaithersburg, MD, 2005 (http://srdata.nist.gov/cccbdb/).

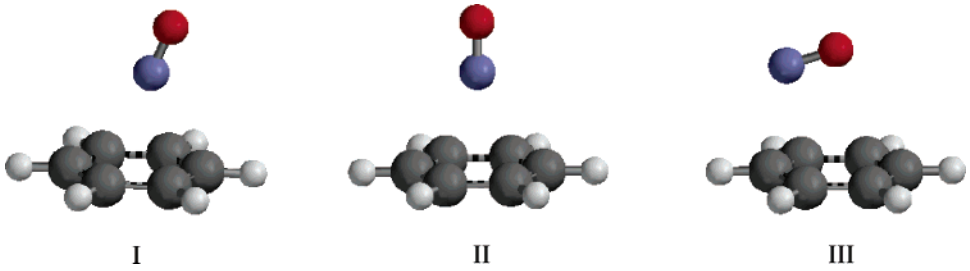

Figure 2. π-Complex structures for [benzene,NO]$^+$ according to B3LYP/6-311+G** calculations.

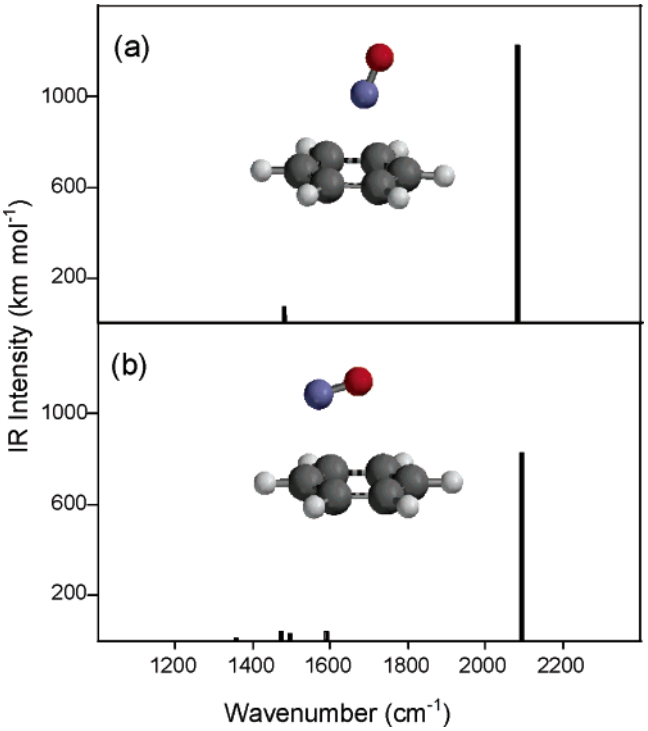

Figure 3. IR spectra for π-complexes **I** (a) and **III** (b) computed at the B3LYP/6-311+G** level. Calculated frequencies are scaled by a factor of 0.98.

though this dependence is frequently observed,[15b,16f] except when the IR FEL is in resonance with a strongly IR-active vibrational mode.[16f] To this end, it is useful to examine the IRMPD feature at 1963 cm^{-1} in Figure 1, associated with a strongly active NO stretching mode. This feature shows clear saturation effects in profile (a). Still, in profiles (b) and (c), which were obtained at the reduced power of 150 and 50 mW, respectively, the relative response does not yet quite reflect the 3:1 ratio of laser power. Saturation effects have been reported and described in the case of transition metal carbonyl complexes, $Fe(CO)_5^+$,[16f] which also display a large infrared absorption cross-section, namely, the ones associated with the CO stretches. Interestingly, the smaller feature at 2040 cm^{-1} appears to be much more linear with respect to intensity over the three power levels.

IRMPD Spectrum of [Benzene,NO]$^+$: Details in the 1700−2100 cm^{-1} Region. The characteristic, strong feature at 1963 cm^{-1} presents a shoulder at 2040 cm^{-1} which becomes an almost resolved peak of about 15% intensity with respect to the parent band in the IRMPD spectrum run at lowest laser power (profile (c) in Figure 1). This feature does not find any correspondence with an active mode in the IR spectrum of the [benzene,NO]$^+$ π-complex **I** nor in any other one calculated for conceivable isomers. Combination bands have been recently reported in the vibrational predissociation spectra of hydrogen bihalide anion clusters and in the IRMPD spectrum of the protonated water dimer in the gas phase.[14b,32] In the present case, one may notice that a bending mode of the NO group in π-complex **I** is calculated at 64 cm^{-1}, which is of the same order of magnitude as 77 cm^{-1}, namely, the difference between 2040 and 1963 cm^{-1}. One may thus be tempted to assign the shoulder at 2040 cm^{-1} to a combination of the strongly active NO stretching mode, which should be anharmonically coupled with the low-energy bending mode of the NO group within π-complex **I**. In order to gain insight into the possible vibrational mode giving rise to this IRMPD feature, an IRMPD spectrum was recorded on a deuterium-labeled ion, namely, [d_6-benzene,-NO]$^+$. The ion was formed by the same route used for the unlabeled species except for the use of d_6-benzene in place of the unlabeled compound. The IRMPD spectrum of [d_6-benzene, NO]$^+$ failed to display any feature at 2040 cm^{-1} (Figure 5). The strong band was hardly perturbed, displaying a maximum at 1950 cm^{-1}, as expected for a mode involving exclusively N−O stretching, whereas the in-plane C-ring distortion was shifted at 1313 cm^{-1} (Table 2). The significance of the 2040 cm^{-1} feature in the IRMPD spectrum of the unlabeled ion thus remains difficult to understand, although it is clearly not due to a combination mode involving exclusively the NO group, which should not be strongly affected by the H/D isotopic substitution. In a further attempt to interpret this feature, calculations (not reported) on a triplet [benzene,NO]$^+$ complex, already characterized by previous computational work,[11] have shown that the presence of this species is not likely to account for a band at 2040 cm^{-1} because the NO stretching mode appears at considerably lower wavenumber. Any formation of triplet [benzene,NO]$^+$, significantly higher in energy than the singlet,[11] appears unlikely also based on the route that was used to form the ion.

One further detail that may be noticed in the IRMPD spectra of both [benzene,NO]$^+$ and [d_6-benzene,NO]$^+$ (Figures 1 and 5) is a weak feature at the common wavenumber of ca. 1742 cm^{-1}. Inspecting the calculated IR spectra of the several possible isomers that were considered, only *para*-protonated nitrosobenzene displays a quite active mode at 1745 cm^{-1} associated with a N−O stretching vibration that could account for the observed feature, unaltered by isotopic substitution. If this assignment were correct, this observation would provide evidence for the formation of a covalent N−C bond as a result of a gas phase cationic nitrosation reaction of benzene, albeit to nearly

(32) (a) Nee, M. J.; Osterwalder, A.; Neumark, D. M.; Kaposta, C.; Cibrián Uhalte, C.; Carter, S.; Asmis, K. R. *J. Chem. Phys.* **2004**, *121*, 7259−7268. (b) Pivonka, N. L.; Kaposta, C.; Brümmer, M.; von Helden, G.; Meijer, G.; Wöste, L.; Neumark, D. M.; Asmis, K. R. *J. Chem. Phys.* **2003**, *118*, 5275−5278.

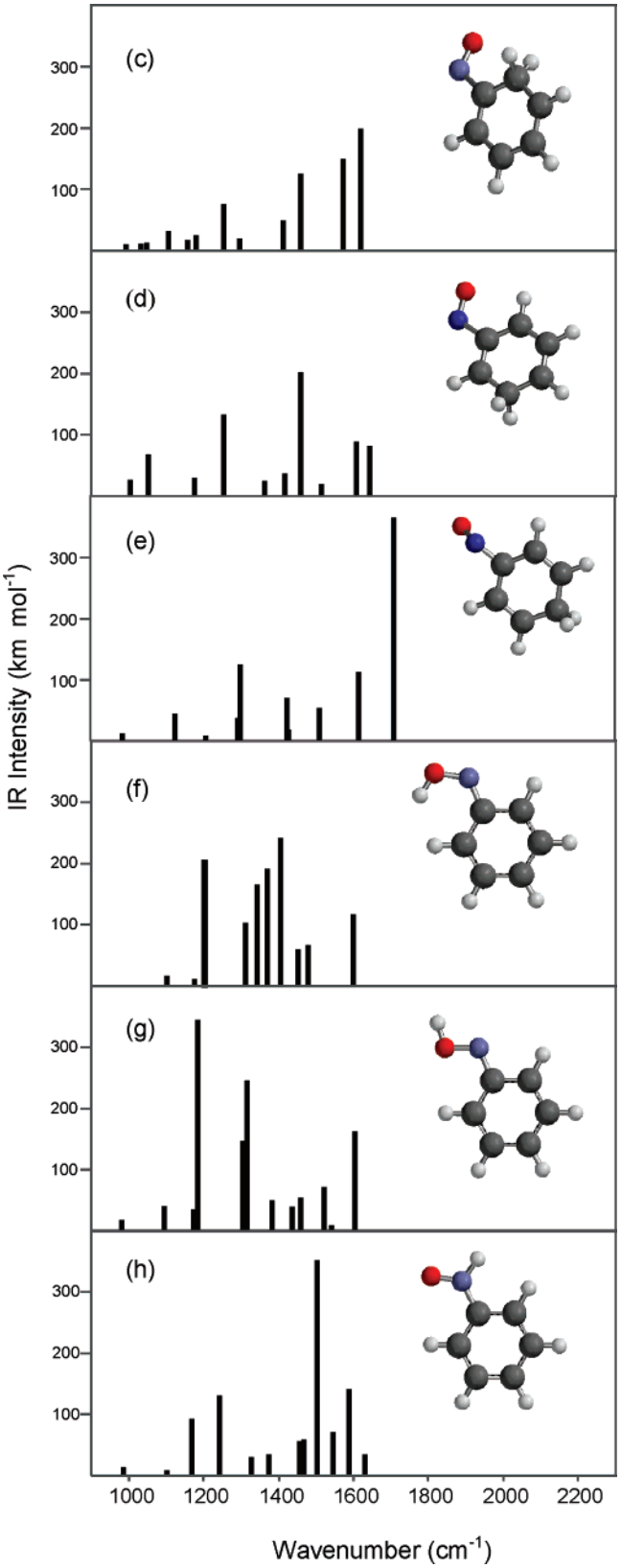

Figure 4. IR spectra of covalently bound $[C_6H_6NO]^+$ isomers (c−h) computed at the B3LYP/6-311+G** level. Calculated frequencies are scaled by a factor of 0.98.

negligible extent. Alternatively, this weak feature at 1742 cm^{-1} could also be the result of a multiphotonic absorption in resonance with a combination of vibrational modes of [benzene,-NO]$^+$.

IRMPD of Protonated Nitrosobenzene. By proving the π-complex structure of [benzene,NO]$^+$ ions obtained by NO^+ transfer to benzene, IRMPD spectroscopy has shown at the same time that in the gas phase this route does not lead to an intermediate prone to evolve to protonated nitrosobenzene by N−C bond formation, supporting previous evidence.[6−8,11] Indeed, the activation energy for the system to proceed to covalent N−C bond formation is predicted to be higher than the dissociation threshold.[2f,4] However, an alternative route to an ionic intermediate resembling a protonated nitrosobenzene species, presumably lying on the reaction coordinate for the nitrosation of benzene, was sought in order to verify the ability of IRMPD to discriminate between $[C_6H_6NO]^+$ isomers. To this end, a quite different source of $[C_6H_6NO]^+$ ions was exploited, based on the protonation of nitrosobenzene, the transfer of ESI-formed ions into a modified Bruker Esquire Paul ion trap, and their assay by IRMPD in the gas phase. The ensuing species show a remarkable difference in their IRMPD behavior compared to the [benzene,NO]$^+$ complex. Figure 6 shows the IRMPD spectrum in the wavenumber range from 800 to 2100 cm^{-1} with a laser power varying from 0.65 to 0.56 W using a single macropulse from the FEL operating at 42 or 45 MeV. Viewing the experimental IRMPD spectrum against the calculated IR spectra shown in Figures 3 and 4 and the experimental IRMPD spectrum of [benzene,NO]$^+$ in Figure 1 clearly suggests that the $[C_6H_6NO]^+$ ions corresponding to protonated nitrosobenzene are species distinct from [benzene,NO]$^+$ complexes. The IRMPD spectrum shown in Figure 6 displays one prominent feature at 1456 cm^{-1}. Four other IRMPD bands were also observed in the low wavenumber portion of the spectrum: two strong features at 1180 and 1252 cm^{-1}, and two weaker bands at 980 and 1350 cm^{-1}. The tentative assignments of the observed features to the calculated transitions are summarized in Table 3. As in Table 2, also in Table 3 the frequencies of the computed IR transitions are scaled by 0.98 and, in a separate column, are given also as raw data. As can be seen in Table 3, the positions of the two bands observed at 1180 and 1252 cm^{-1} nicely match with the calculated positions of two calculated modes of the N-protonated isomer at 1169 and 1242 cm^{-1} associated with strong intensities (90 and 130 km mol^{-1}, respectively). Furthermore, the observation of the two weaker features at 980 and 1350 cm^{-1} could also be the result of the resonant absorption through the vibrational modes of N-protonated nitrosobenzene calculated at 975 and 1329 cm^{-1}. Once again, it is noteworthy that, despite the multiphotonic character of the absorption process associated with the IRMPD, the relative intensities of the four observed bands at 980, 1180, 1252, and 1350 cm^{-1} are comparable to the ones calculated for the IR absorption spectrum of the N-protonated nitrosobenzene. As in the IRMPD spectrum (Figure 6), which is dominated by a prominent feature observed at 1456 cm^{-1}, the calculated IR absorption spectrum of the N-protonated isomer displays a strong band and several closely spaced IR-active modes ranging from 1475 and 1632 cm^{-1} (Table 3). All these in-plane vibrational modes result from the coupling of CH/NH bendings, ring deformations, and NO stretching. At our level of calculation, the most intense IR-active bands, displaying a strong NO stretching component, is predicted at 1502 cm^{-1} (350 km mol^{-1}). Once again, the raw frequency value of this specific type of vibrational mode requires a factor of 0.95 (see ratio exp/theory

Table 2. Major Vibrational Modes of [Benzene,NO]$^+$ and Model Species in the 1100−2400 cm^{-1} Region[a]

species	IR mode[b]	exptl IR	exptl IRMPD[c]	theory[d]	theory[e] (scaled)	ratio exp/theory
benzene	σ_{CC}, β_{CH}	1486[f]		1511 (14)	1481	0.983
d_6-benzene	σ_{CC}, β_{CD}	1335[f]		1358 (2)	1331	0.983
NO	σ_{NO}	1876[g]		1981 (46)	1941	0.947
NO^+	σ_{NO}	2344[h]		2490 (31)	2440	0.941
[benzene,NO]$^+$	σ_{CC}, β_{CH}		1467 (0.06)	1501 (64)	1471	0.977
[benzene,NO]$^+$			1742 (∼0.004)			
[benzene,NO]$^+$	σ_{NO}		1963 (1.00)	2117 (1220)	2075	0.927
[benzene,NO]$^+$			2040 (0.16)			
[d_6-benzene,NO]$^+$	σ_{CC}, β_{CD}		1313 (0.04)	1339 (38)	1312	0.981
[d_6-benzene,NO]$^+$			1743 (∼0.004)			
[d_6-benzene,NO]$^+$	σ_{NO}		1950 (1.00)	2116 (1217)	2074	0.922

[a] Vibrational wavenumbers are given in cm^{-1}. [b] β = in-plane bend; σ = stretch. [c] Relative IRMPD yields are given in parentheses. [d] B3LYP/6-311+G**. No scaling factors are employed. IR intensities (in parentheses) in km mol^{-1}. [e] A scaling factor of 0.98 is applied to the calculated frequencies. [f] From ref 28. [g] From ref 29. [h] From refs 29 and 30.

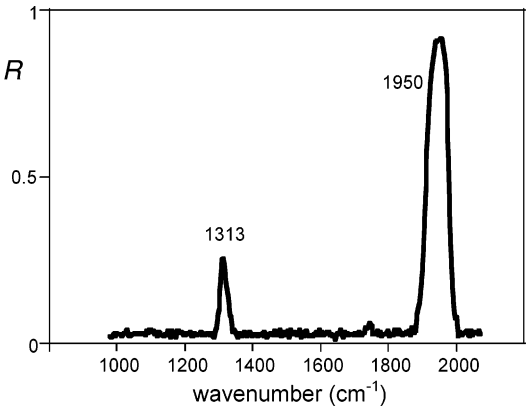

Figure 5. IRMPD spectrum of [d_6-benzene,NO]$^+$.

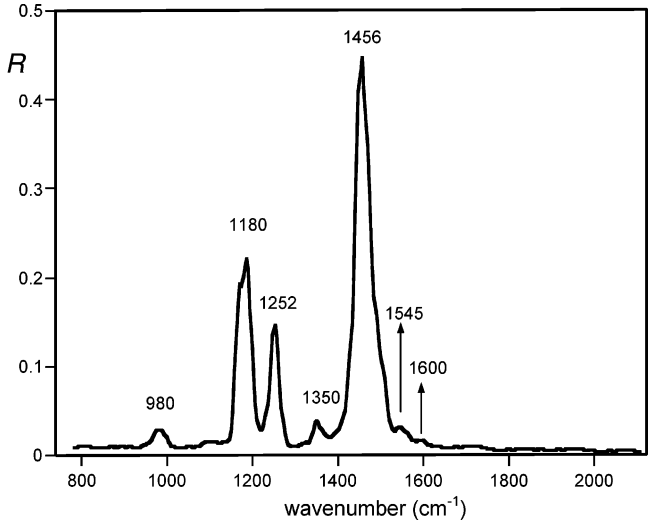

Figure 6. IRMPD spectrum of protonated nitrosobenzene.

in Table 3) to match with the prominent experimental feature at 1456 cm^{-1}. It should be noted however that the relative intensities of closely spaced normal modes resulting from the coupling of local modes have to be taken with extreme caution. As a matter of fact, the relative intensities of the IR-active modes in the 1400−1680 cm^{-1} range strongly depend on the choice of hybrid density functional (B3LYP, B3P86, or B3PW91). Any contribution of the *trans*-O-protonated species, which is in fact only 8.5 kJ mol^{-1} higher in energy relative to the N-protonated species, is unlikely because the IR absorption spectrum of the *trans*-O-protonated isomer displays a strong feature at 1317 cm^{-1}, in a region where no strong IRMPD features were observed experimentally. Furthermore, the *trans*-O-protonated species also displays a distinct absorption band at 805 cm^{-1} (92 km mol^{-1}), whereas no significant photofragmentation was observed in this wavenumber range.

Table 3. Major IRMPD Features of Protonated Nitrosobenzene and Calculated IR Modes in the 800−2400 cm^{-1} Region[a]

theory for $C_6H_5N(H)O^+$ [b]	theory[c] (scaled)	exptl IRMPD[d]	ratio exp/theory
995 (36) (β'_{CH}, β'_{NH})	975	980 (0.05)	0.985
1193 (90) (β_{CH})	1169	1180 (0.50)	0.989
1267 (130) (σ_{CN}, β_{CH})	1242	1252 (0.32)	0.988
1356 (29) (σ_{CN},β_{CH})	1329	1350 (0.05)	0.996
1403 (33) (σ_{CC})	1375		
1486 (54) (σ_{CC}, β_{CH})	1456		
1498 (57) (σ_{CC}, β_{CH})	1468		
1533 (350) (σ_{NO}, β_{NH})	1502	1456 (1.00)	0.950
1578 (68) (σ_{NO}, σ_{CC}, β_{CH})	1546	1545 (0.05)	0.979
1621 (140) (σ_{CC}, β_{NH})	1589	1599 (0.03)	0.986
1665 (32) (σ_{NO}, σ_{CC}, β_{CH})	1632		

[a] Vibrational wavenumbers are given in cm^{-1}. [b] B3LYP/6-311+G**. No scaling factors are employed. IR intensities (in parentheses) in km mol^{-1}. β = in-plane bend; β' = out-of-plane bend; σ = stretch. [c] A scaling factor of 0.98 is applied to the calculated frequencies. [d] Relative IRMPD yields are given in parentheses.

$[C_6H_5N(H)O]^+$ ions are characterized not only by their IRMPD spectrum but also by a specific fragmentation motif, not shown by the [benzene,NO]$^+$ isomer. In correspondence with the major IRMPD feature at 1456 cm^{-1}, they show a decomposition path by OH loss (ca. 20% with respect to NO loss), as conceivable from a $[C_6H_5N(H)O]^+$ bonding network.

In contrast with the distinct difference in their IRMPD behavior, it may be noted that the high-energy CID mass spectra of [benzene,NO]$^+$ and protonated nitrosobenzene in a multiple sector instrument were found to be closely similar.[11]

Conclusions

Gaseous [benzene,NO]$^+$ π-complexes have been characterized by IRMPD spectroscopy, relying on the wavelength-dependent photodissociation process activated by the absorption of multiple monochromatic photons. The experimental IRMPD spectrum in the 1100−2200 cm^{-1} range is characterized by two prominent features that are found to match with the absorption bands in the calculated IR spectrum of a "perpendicular"-type structure **I**. The complex is formed by a formal NO^+ transfer reaction and does not evolve into the thermodynamically favored isomer corresponding to N-protonated nitrosobenzene, at least

to any significant extent. The latter species is preferentially formed by protonation of nitrosobenzene as obtained by ESI of a methanol solution. $[C_6H_5N(H)O]^+$ ions are unambiguously discriminated from the [benzene,NO]$^+$ isomers when subjected to assay by IRMPD.

The IR absorption features for the [benzene,NO]$^+$ gaseous species disclosed by the IRMPD spectrum may be examined with respect to the NO stretching frequency data reported for the similar complex formed in nitromethane solution. Both the $\nu_{NO} = 2075$ cm^{-1} value for the complex in solution[2a] and the $\nu_{NO} = 1963$ cm^{-1} frequency for the gaseous species are in between the stretching frequencies of NO$^\bullet$ (1876 cm^{-1})[29] and NO$^+$ (2344 cm^{-1}),[29,30] suggesting that the positive charge is distributed between the NO group and the aromatic moiety.[2] The gaseous π-complex is expected to adiabatically dissociate to $C_6H_6^{+\bullet}$,[11] the observed photofragmentation product. The IRMPD characterization of gaseous [benzene,NO]$^+$ has thus provided information on the prototypical model for the strong noncovalent (charge transfer) interactions established between nitric oxide and the π-electron systems of calixarenes[33] and, possibly, of biomolecules.

The present [benzene,NO]$^+$ π-complex shares some features in common with transition metal ion−benzene complexes, whose IRMPD behavior has been thoroughly described.[16c,d] The in-plane carbon ring distortion band at 1486 cm^{-1} for benzene is typically shifted to lower frequency in the M(benzene)$^+$ complexes (1425−1444 cm^{-1}, M = V, Co, Ni). The red shift is considered to be an indicator for the degree of metal−benzene charge transfer interaction.[16d] The corresponding IRMPD band of [benzene,NO]$^+$ is red shifted at 1467 cm^{-1}, thus confirming a character of charge transfer complex.

As a final comment, the IRMPD methodology exploiting the CLIO-FEL IR radiation source coupled to FT-ICR and to Paul ion trap mass spectrometry has proven to be a valuable tool in characterizing the manifold ionic species that may originate from the attack of a positively charged electrophile to a simple aromatic molecule. These species include arenium ions or σ-complexes (as obtained from the protonation of benzene, fluorobenzene, toluene),[34] *ipso*-type arenium ions (the most stable isomer of protonated phenylsilane),[35] and π-complexes (the present [benzene,NO]$^+$ complex) besides substituent-protonated species (protonated benzaldehyde[36] and, presently, protonated nitrosobenzene). Using a related approach based on the IR photodissociation of molecular clusters (so-called messenger technique), ionic clusters of aromatic molecules have been thoroughly examined in the OH and CH stretch regions.[37] In this way, exploiting different IR photodissociation techniques, one may gain an in-depth understanding of the gas phase ion chemistry of simple aromatic molecules.

Acknowledgment. This work was supported by the CNRS, the laser center POLA at the Université Paris-Sud 11, and the Italian MIUR. We thank Jean-Michel Ortega and the CLIO team for their support during the experiments. We also thank Gérard Mauclaire, Michel Heninger, Gerard Bellec, and Pierre Boissel who, together with one of us (J.L.), provided us with the mobile FT-ICR mass spectrometer used in this work. Financial support by the European Commission is gratefully acknowledged.

Note Added after ASAP Publication. Due to a production error, the unit for the calculated intensities was incorrectly given as kJ mol^{-1} in the *y*-axis labels of Figures 3 and 4, in the footnotes of Tables 2 and 3, and in the first paragraph under the heading "IRMPD of Protonated Nitrosobenzene" in the Results and Discussion section in the version of this paper published ASAP on September 2, 2006. The correct unit is km mol^{-1}. The corrected version was published ASAP on September 7, 2006.

JA0637548

(33) (a) Rathore, R.; Lindeman, S. V.; Rao, K. S. S. P.; Sun, D.; Kochi, J. K. *Angew. Chem., Int. Ed.* **2000**, *39*, 2123−2127. (b) Rathore, R.; Lindeman, S. V.; Kochi, J. K. *Angew. Chem., Int. Ed.* **1998**, *37*, 1585−1587.

(34) (a) Jones, W.; Boissel, P.; Chiavarino, B.; Crestoni, M. E.; Fornarini, S.; Lemaire, J.; Maître, P. *Angew. Chem., Int. Ed.* **2003**, *42*, 2057−2059. (b) Dopfer, O.; Solcà, N.; Lemaire, J.; Maître, P.; Crestoni, M. E.; Fornarini, S. *J. Phys. Chem. A* **2005**, *109*, 7881−7887. (c) Dopfer, O.; Lemaire, J.; Maître, P.; Chiavarino, B.; Crestoni, M. E.; Fornarini, S. *Int. J. Mass Spectrom.* **2006**, *249*−*250*, 149−154.

(35) Chiavarino, B.; Crestoni, M. E.; Fornarini, S.; Lemaire, J.; MacAleese, L.; Maître, P. *ChemPhysChem* **2005**, *6*, 437−440.

(36) Chiavarino, B.; Crestoni, M. E.; Fornarini, S.; Dopfer, O.; Lemaire, J.; Maître, P. *J. Phys. Chem. A* **2006**, *110*, 9352−9360.

(37) (a) Solcà, N.; Dopfer, O. *Angew. Chem., Int. Ed.* **2002**, *41*, 3628−3631. (b) Solcà, N.; Dopfer, O. *Angew. Chem., Int. Ed.* **2003**, *42*, 1537−1540. (c) Solcà, N.; Dopfer, O. *J. Am. Chem. Soc.* **2004**, *126*, 1716−1725. (d) Solcà, N.; Dopfer, O. *J. Chem. Phys.* **2004**, *120*, 10470−10482. (e) Solcà, N.; Dopfer, O. *ChemPhysChem* **2005**, *6*, 434−436. (f) Yeh, L. I.; Okumura, M.; Myers, J. D.; Price, J. M.; Lee, Y. T. *J. Chem. Phys.* **1989**, *91*, 7319−7330. (g) Okumura, M.; Yeh, L. I.; Myers, J. D.; Lee, Y. T. *J. Chem. Phys.* **1986**, *85*, 2338−2329. (h) Fujii, A.; Fujimaki, E.; Ebata, T.; Mikami, N. *J. Chem. Phys.* **2000**, *112*, 6275−6284.